

Heterolytic Benzene C–H Activation by a Cyclometalated Iridium(III) Dihydroxo Pyridyl Complex: Synthesis, Hydrogen–Deuterium Exchange, and Density Functional Study

Steven K. Meier,[†] Kenneth J. H. Young,[†] Daniel H. Ess,^{§,‡} William J. Tenn, III,[†] Jonas Oxgaard,[‡] William A. Goddard, III,^{*,‡} and Roy A. Periana^{*,†,§}

[†]Department of Chemistry, Loker Hydrocarbon Institute, University of Southern California, Los Angeles, California 90089, [§]Department of Chemistry, The Scripps Research Institute, Jupiter, Florida 33458, and [‡]Materials and Process Simulation Center, Beckman Institute (139-74), Division of Chemistry and Chemical Engineering, California Institute of Technology, Pasadena, California 91125.

Received January 17, 2009

We report the synthesis of the pincer-cyclometalated (NNC^{t-Bu})Ir(III) dihydroxo pyridyl complex **6**, which catalyzes hydrogen–deuterium (H/D) exchange between water and benzene in the presence of base (TOF = $\sim 6 \times 10^{-3} \text{ s}^{-1}$ at 190 °C). Experimental and density functional theory (B3LYP) studies suggest that H/D exchange occurs through loss of pyridine followed by benzene coordination and C–H bond activation by a heterolytic substitution mechanism to give a phenyl aquo complex, which may dimerize. Exchange of H₂O for D₂O followed by the microscopic reverse of CH activation leads to deuterium incorporation into benzene. Synthesis of the μ -hydroxo phenyl dinuclear complex [(NNC^{t-Bu})Ir(Ph)(μ -OH)]₂ (**9**) also catalyzes H/D exchange with a turnover frequency (TOF = $\sim 7 \times 10^{-3} \text{ s}^{-1}$ at 190 °C) similar to that for **6**.

Introduction

Hydrocarbon CH activation followed by heteroatom functionalization has great potential for installing diverse functionality into C–H bonds.¹ The most efficient hydrocarbon hydroxylation catalysts utilize platinum, palladium, mercury, and gold complexes and operate by a sequence of electrophilic C–H bond activation² followed by reductive functionalization to generate the C–OR functionality. Because of their electrophilic character, these previous generations of hydroxylation catalysts are highly susceptible to water and alcohol inhibition and therefore require strong acid solvents to minimize this inhibition.^{2a}

To thwart this inhibition, we decided to modify the highly effective Pt(bipyrimidine)L₂ motif into a less electrophilic³ catalyst by increasing the electron density at the metal center

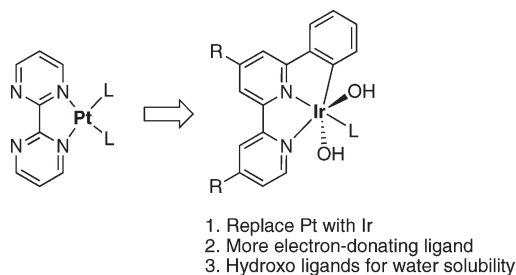


Figure 1. Progression toward less electrophilic CH activation catalysts.

by using a more electron donating ligand and replacing platinum with iridium (Figure 1). Previously, our group reported the synthesis of a Pt(NNC^{t-Bu})TFA complex (NNC^{t-Bu} = 6-phenyl-4,4'-di-*tert*-butyl-2,2'-bipyridine and TFA = trifluoroacetate) that promotes H/D exchange of benzene and trifluoroacetic acid with an activation barrier of $\sim 30 \text{ kcal/mol}$.^{3c} More importantly, we have recently reported that the (NNC^{t-Bu})Ir(TFA)₂(C₂H₄) complex catalytically activates and functionalizes methane in trifluoroacetic acid.⁴ This system was developed on the basis of the results that treatment of (NN)(NC)Ir^{III}(Me)OTf (NN = κ^2 -4,4'-di-*tert*-butyl-2,2'-bipyridine, NC = κ^2 -(*N,C*-3)-6-phenyl-2,2'-bipyridine, OTf = trifluoromethanesulfonate) with PhI-(TFA)₂ (PITFA) results in efficient oxy functionalization to generate the methyl ester.⁵

*To whom correspondence should be addressed. E-mail: rperiana@scripps.edu (R.A.P.); wag@wag.caltech.edu (W.A.G.).

(1) (a) Labinger, J. A.; Bercaw, J. E. *Nature* **2002**, *417*, 507. (b) Waltz, K. M.; Hartwig, J. F. *Science* **1997**, *277*, 211. (c) Crabtree, R. H. *Dalton Trans.* **2001**, 2951. (d) Conley, B. L.; Tenn, W. J., III; Young, K. J. H.; Ganesh, S. K.; Meier, S. K.; Ziatdinov, V. R.; Mironov, O. A.; Oxgaard, J.; Gonzales, J.; Goddard, W. A., III; Periana, R. A. *J. Mol. Catal. A* **2006**, *251*, 8.

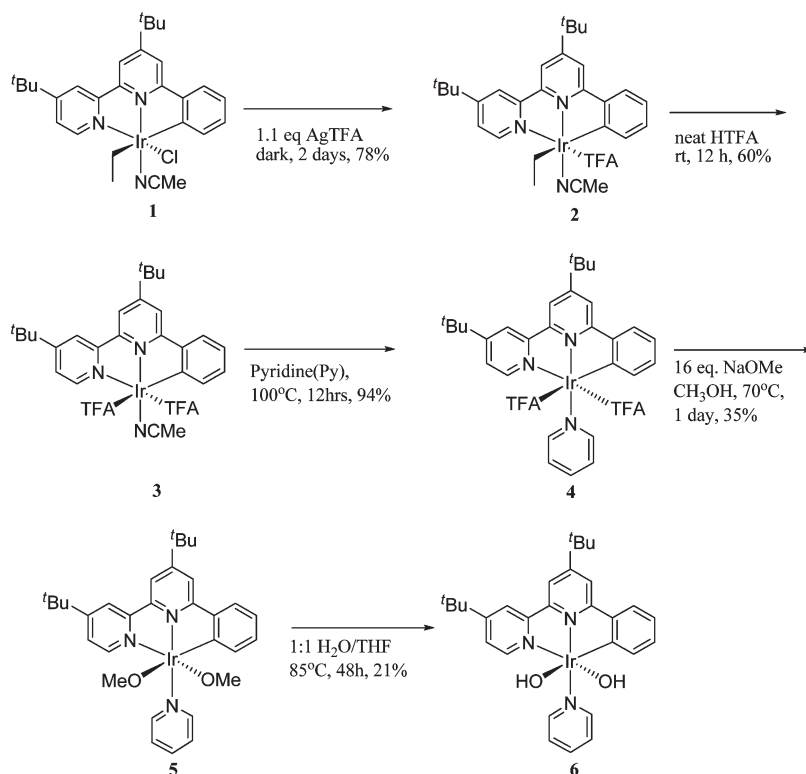
(2) (a) Periana, R. A.; Taube, D. J.; Gamble, S.; Taube, H.; Satoh, T.; Fujii, H. *Science* **1998**, *280*, 560. (b) Periana, R. A.; Mironov, O.; Taube, D. J.; Bhalla, G.; Jones, C. J. *Science* **2003**, *301*, 814. (c) Periana, R. A.; Taube, D. J.; Evtitt, E. R.; Loffler, D. G.; Wentreck, P. R.; Voss, G.; Masuda, T. *Science* **1993**, *259*, 340. (d) Jones, C. J.; Taube, D.; Ziatdinov, V. R.; Periana, R. A.; Nielsen, R. J.; Oxgaard, J.; Goddard, W. A., III *Angew. Chem., Int. Ed.* **2004**, *43*, 4626. (e) Periana, R. A.; Mironov, O. A.; Taube, D. J.; Gamble, S. *Chem. Commun.* **2002**, 2376.

(3) (a) Zhong, H. A.; Labinger, J. A.; Bercaw, J. E. *J. Am. Chem. Soc.* **2002**, *124*, 1378. (b) Periana, R. A.; Bhalla, G.; Tenn, W. J., III; Young, K. J. H.; Liu, X. Y.; Mironov, O. A.; Jones, C. J.; Ziatdinov, V. R. *J. Mol. Catal. A* **2004**, *220*, 7. (c) Young, K. J. H.; Meier, S. K.; Gonzales, J. M.; Oxgaard, J.; Goddard, W. A., III; Periana, R. A. *Organometallics* **2006**, *25*, 4734.

(4) Young, K. J. H.; Oxgaard, J.; Ess, D. H.; Meier, S. K.; Stewart, T.; Goddard, W. A., III; Periana, R. A. *Chem. Commun.* **2009**, 3270.

(5) (a) Young, K. J. H.; Mironov, O. A.; Periana, R. A. *Organometallics* **2007**, *26*, 2137. (b) Young, K. J. H.; Yousufuddin, M.; Ess, D. H.; Periana, R. A. *Organometallics* **2009**, *28*, 3395.

Scheme 1. Synthesis of 6



Several groups have developed systems that are competent for CH activation in aqueous or mixed organic/aqueous media. The most well-known system that operates in water is the Shilov⁶ catalyst that uses K_2PtCl_4 . Gunnoe⁷ and Lau⁸ in separate work have also demonstrated that ruthenium hydro(trispyrazolyl)borate complexes promote H/D exchange between water and arene substrates. More examples include the work of Milstein and Leitner,⁹ who utilized a ruthenium pincer complex, the classic Bergman¹⁰ (Cp)-Ir(PMe₃)Cl₂ complex, and more recently Goldberg's¹¹ (PNP)Rh(OPh) complex. Carmona and Poveda¹² have also shown that H/D exchange occurs between tetrahydrofuran and water using a (Tp^{Me2})IrH₄ catalyst (Tp^{Me2} = hydro(tris-(3,5-dimethylpyrazolyl)borate). In addition, our own work

previously showed that the (κ^2 -O,O-acac)₂Ir(OH)(OH)₂ complex (acac = acetylacetonate) catalyzes H/D exchange between benzene and water.¹³

Here we report the synthesis and experimental study of benzene and water H/D exchange catalyzed by a dihydroxo iridium(III) pyridine complex, (NNC^{t-Bu})Ir(OH)₂Py (**6**). Density functional calculations are also reported that were used to explore several possible mechanisms for H/D exchange.

Results and Discussion

Synthesis. Scheme 1 shows the synthesis of the (NNC^{t-Bu})Ir(OH)₂Py complex. With (NNC^{t-Bu})Ir(Et)(Cl)NCCH₃ (**1**)⁴ as the starting material, the chloride was replaced with the more labile trifluoroacetate group by stirring complex **1** for 2 days in the presence of silver trifluoroacetate to yield (NNC^{t-Bu})Ir(Et)(TFA)NCCH₃ (**2**) in 78% yield after recrystallization. The ethyl group was also replaced by stirring complex **2** under argon in neat trifluoroacetic acid for 12 h at room temperature. After removal of the acid under reduced pressure and purification by column chromatography, a yellow, air-stable solid was obtained in 60% yield as the complex (NNC^{t-Bu})Ir(TFA)₂NCCH₃ (**3**). Fluorine NMR analysis shows only one fluorine resonance, suggesting that the trifluoroacetate groups are oriented trans to one another. Direct routes to (NNC^{t-Bu})Ir(OH)₂L (L = H₂O, NCCH₃) were unsuccessful, due to the insolubility of **3** in water. Therefore, the trifluoroacetate ligands were replaced with methoxo ligands, since we knew that **3** was soluble in methanol. The dimethoxo precursor complex was advantageous because the dimethoxo product can easily be identified by ¹H NMR due to the presence of the methyl protons of the methoxo groups. The reaction of **3** in methanol with 16 equiv of sodium methoxide was followed by ¹H NMR. After the

(6) (a) Goldshleger, N. F.; Tyabin, M. B.; Shilov, A. E.; Shteinman, A. A. *Zh. Fiz. Khim.* **1969**, *43*, 2174. (b) Shilov, A. E.; Shteinman, A. A. *Coord. Chem. Rev.* **1977**, *24*, 97.

(7) (a) Feng, Y.; Lail, M.; Barakat, K. A.; Cundari, T. R.; Gunnoe, T. B.; Petersen, J. L. *J. Am. Chem. Soc.* **2005**, *127*, 14174. (b) Feng, Y.; Lail, M.; Foley, N. A.; Gunnoe, T. B.; Barakat, K. A.; Cundari, T. R.; Petersen, J. L. *J. Am. Chem. Soc.* **2006**, *128*, 7982.

(8) Leung, C. W.; Zheng, W.; Wang, D.; Ng, S. M.; Yeung, C. H.; Zhou, Z.; Lin, Z.; Lau, C. P. *Organometallics* **2007**, *26*, 1924.

(9) Precht, M. H. G.; Hölscher, M.; Ben-David, Y.; Theysen, N.; Loshcen, R.; Milstein, D.; Leitner, W. *Angew. Chem., Int. Ed.* **2007**, *46*, 2269.

(10) (a) Klei, S. R.; Golden, J. T.; Tilley, T. D.; Bergman, R. G. *J. Am. Chem. Soc.* **2002**, *124*, 2092. (b) Klei, S. R.; Tilley, T. D.; Bergman, R. G. *Organometallics* **2002**, *21*, 4905.

(11) (a) Kloek, S. M.; Heinekey, D. M.; Goldberg, K. I. *Angew. Chem., Int. Ed.* **2007**, *46*, 4736. (b) Hanson, S. K.; Heinekey, D. M.; Goldberg, K. I. *Organometallics* **2008**, *27*, 1454.

(12) Gutiérrez-Puebla, E.; Monge, A.; Paneque, M.; Poveda, M. L.; Taboada, S.; Trujillo, M.; Carmona, E. *J. Am. Chem. Soc.* **1999**, *121*, 346.

(13) (a) Tenn, W. J., III; Young, K. J. H.; Bhalla, G.; Oxgaard, J.; Goddard, W. A., III; Periana, R. A. *J. Am. Chem. Soc.* **2005**, *127*, 14172. (b) Tenn, W. J., III; Young, K. J. H.; Oxgaard, J.; Nielsen, R. J.; Goddard, W. A., III; Periana, R. A. *Organometallics* **2006**, *25*, 5173.

Table 1. Percentage of Benzene Isotopologues Resulting from Control (Left) and Catalytic (Right) Reactions at 180 °C^a

control reaction ^b			catalytic reaction ^c				
isotopologue	277 min	1980 min	3060 min	isotopologue	277 min	1980 min	3060 min
C ₆ H ₆	99.9	99.7	99.04	C ₆ H ₆	99.81	90.67	87.62
C ₆ H ₅ D ₁	0	0.24	0.93	C ₆ H ₅ D ₁	0.15	8.91	11.77
C ₆ H ₄ D ₂	0	0	0	C ₆ H ₄ D ₂	0.01	0.38	0.55
C ₆ H ₃ D ₃	0	0	0	C ₆ H ₃ D ₃	0	0.01	0.04
C ₆ H ₂ D ₄	0	0	0	C ₆ H ₂ D ₄	0	0	0
C ₆ H ₁ D ₅	0	0	0	C ₆ H ₁ D ₅	0	0	0
C ₆ D ₆	0	0	0	C ₆ D ₆	0	0	0

^a Concentrations are given on the basis of total volume of solution present. ^b H/D exchange analysis. Conditions: 0.16 M KOD, 0.5 mL of D₂O, 0.5 mL of benzene-H₆. ^c H/D exchange analysis. Conditions: 2.13 mM of **6**, 0.16 M KOD, 0.5 mL of D₂O, 0.5 mL of benzene-H₆.

addition of the sodium methoxide, the Ir–NCCH₃ peak could no longer be observed by ¹H NMR. Additional heating at 70 °C led to multiple intractable products. The instability of **3** in the presence of base is likely due to the reaction of the NCCH₃ with base. Therefore, NCCH₃ was substituted with a more stable ligand by heating complex **3** in neat pyridine overnight at 100 °C. Unreacted pyridine was removed under reduced pressure, and purification of the product by column chromatography yielded the air-stable orange solid (NNC^{*t*-Bu})Ir(TFA)₂Py (**4**) in 94% yield. Complex **4** was not soluble in water, which ruled out direct routes to a hydroxo complex. Therefore, **4** was heated at 70 °C for 24 h in methanol containing 16 equiv of sodium methoxide. The product, (NNC^{*t*-Bu})Ir(OMe)₂Py (**5**), was obtained by removal of the excess sodium methoxide and methanol, and it was purified by column chromatography, resulting in a black solid in 35% yield. Complex **5** was immediately converted to (NNC^{*t*-Bu})Ir(OH)₂Py (**6**) after purification. Complex **6** was obtained by heating **5** in a 1:1 mixture of THF and H₂O at 85 °C for 2 days. Complex **6** was obtained in 21% yield as a black solid by removal of the solvent and purification by column chromatography. Complex **6** was fully characterized by ¹H and ¹³C NMR, high-resolution mass spectrometry, and elemental analysis. The –OH protons for **6** were observed in the ¹H NMR at δ –2.71 ppm in CDCl₃. Attempts to obtain a crystal structure were unsuccessful.

Stability. The stability of **6** in water was tested by heating a 5.0 mM solution of **6** in D₂O under argon inside of a J. Young NMR tube. As the solution was heated at 100 °C over a period of 8 h, two new species were observed by ¹H NMR (see the Supporting Information), and attempts to isolate these two species by preparative thin-layer chromatography failed. During the course of this reaction the concentration of free pyridine did not increase. Hydroxo ligand loss could not be ruled out. The loss of the hydroxo group could potentially produce a dinuclear species of the type [(NNC^{*t*-Bu})IrPy(μ-OH)]₂⁺ (see Density Functional Theory Investigation). Addition of KOD and further heating did not result in the conversion of the two unknown species back to **6**. The two unknown species produced by heating **6** in H₂O are also observed in the resulting crude mixture from the synthesis of **6**. Hypothesizing that loss of a hydroxide group was resulting in the formation of these byproducts, we repeated the stability reaction in the presence of 4 equiv of KOD. After 2 h at 130 °C only **6** was observed by ¹H NMR (see the Supporting Information). At 150 °C the concentration of **6** slightly decreases relative to an external standard and small amounts of solid were observed on the wall of the NMR tube. Similar studies were also carried out in Schlenk tubes to confirm that the charred material was not produced from the

inability to stir the solution in the NMR tube. The thermal stability tests carried out in Schlenk tubes resulted in precipitation of a tan solid within several hours of heating the solution at 150 °C. ¹H NMR analysis of the tan solid, using deuterated acetone, revealed a broad range of aromatic and *tert*-butyl NMR peaks, indicating a mixture of products.

Catalytic H/D Exchange. Benzene and water H/D exchange was carried out using a 1:1 mixture of benzene-H₆ and D₂O, resulting in an approximately 2.0–3.5 mM solution of catalyst **6**. Deuterium incorporation into benzene was monitored up to 5% deuterium incorporation at 160–190 °C by analysis of the benzene phase by GC-MS using a deconvolution program (see the Experimental Section). Initial H/D exchange studies between water and benzene without added KOD showed little to no H/D exchange over a 48 h period (less than 10 turnovers at 180 °C). Knowing that added base stabilizes **6**, 20 equiv of KOD was added to the reaction mixture. H/D exchange was observed to be steady over time with a turnover frequency (TOF) of 2.0 × 10^{–3} s^{–1} at 180 °C. Control reactions were carried out with the same amount of KOD, and all H/D exchange results are reported with background corrections. Table 1 gives the analysis of the catalytic H/D exchange compared to the background.

Figure 2 shows a stirring rate study for H/D exchange between benzene-H₆ and D₂O using **6** as a catalyst at 190 °C to determine if the reaction was mass transfer limited. The highest temperature used for H/D exchange studies was chosen because the chemical rates would be the most competitive with the rate of diffusion. Figure 2 shows that for the range of 300–1000 rpm the catalyst is not mass transfer limited.¹⁴

Similar turnover frequencies (TOF) were observed for benzene/water H/D exchange with varying amounts of KOD (Figure 3). However, KOD concentration dependence cannot be ruled out, because it appears that the catalyst is operating in the benzene phase, where the amount of base is likely saturated. When the reaction mixture is loaded into a Schlenk flask, the aqueous phase is red due to the presence of the catalyst and the benzene phase is colorless. Once the reaction mixture is heated at 180 °C, the benzene layer turns black. If the reaction is stopped after a short period of time, the benzene phase is black and the aqueous phase is colorless, indicating that the catalyst likely resides in the benzene phase. To further confirm this, we carried out the H/D

(14) However, these stirring studies were performed using PTFE stir bars rather than an overhead-driven stirrer with an impeller. As a result, at high stir rates it is possible that the solution is vortexing rather than efficiently mixing.

exchange of benzene and D₂O using **6**. The reaction was carried out at 190 °C for 17 h, and the benzene phase was completely removed and analyzed by GC-MS, resulting in a TOF of $7.5 \times 10^{-3} \text{ s}^{-1}$ (23.2% C₆H₅D and 2.8% C₆H₄D₂) with the results corrected for background H/D exchange. New benzene containing no catalyst was added to the remaining aqueous solution, and the reaction mixture was

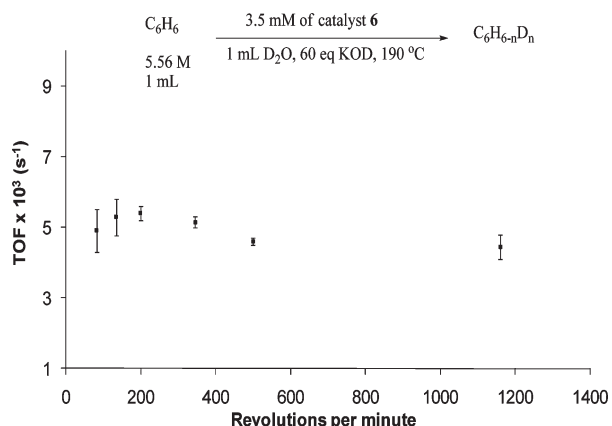


Figure 2. Stirring rate study for H/D exchange between benzene-H₆ and D₂O in the presence of **6**.

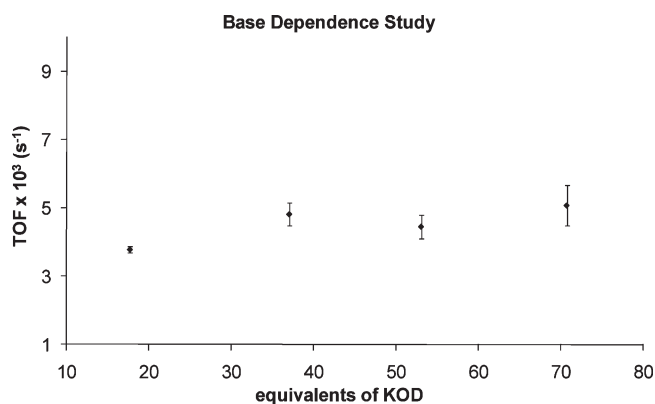


Figure 3. Plot of turnover frequency vs equivalents of KOD. Determination of base dependence on H/D exchange.

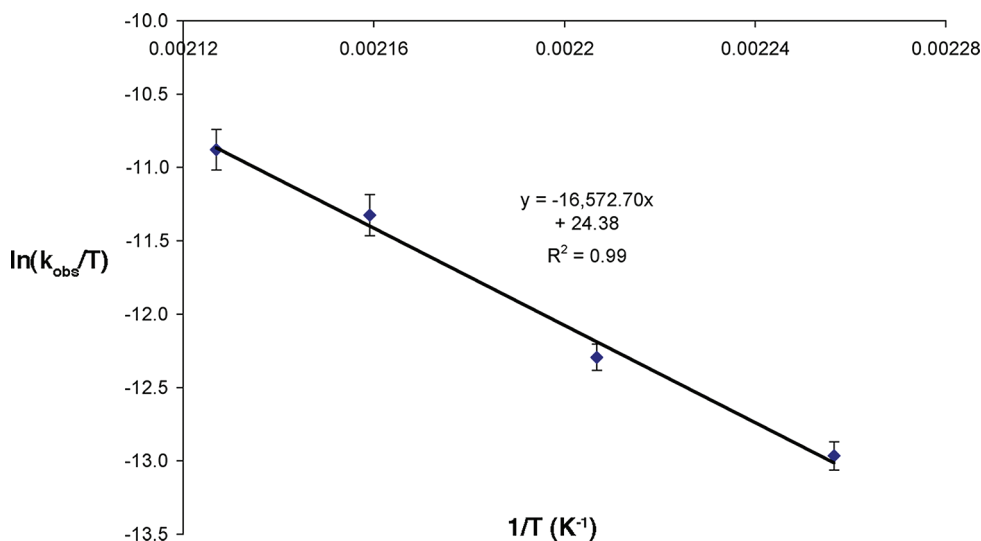


Figure 4. Eyring plot for H/D exchange by **6** with benzene-H₆ and D₂O.

heated for another 17 h at 190 °C under argon. Analysis of the benzene phase showed no H/D exchange, which indicates that no catalyst is present in the aqueous phase.

H/D exchange studies with **6** showed an inverse dependence of pyridine through a $1/[\text{Py}]$ study conducted at 190 °C (see the Supporting Information). Figure 4 shows an Eyring plot for H/D exchange of benzene and water over a temperature range of 160–190 °C. Linear regression analysis gives an activation enthalpy (ΔH^\ddagger) of $33(\pm 2) \text{ kcal/mol}$.

Phenyl Complex. Carrying out the stoichiometric reaction under the catalytic conditions used for H/D exchange yielded multiple products. One of the possible products from C–H activation of benzene is $(\text{NNC}^{t\text{-Bu}})\text{Ir}(\text{Ph})(\text{OH})\text{Py}$ (**7**). Our group previously reported a similar complex, $(\text{NNC}^{t\text{-Bu}})\text{Ir}(\text{Ph})(\text{Cl})\text{Py}$ (**8**), which was used as a precursor for the attempted synthesis of **7** (Scheme 2).⁴ Complex **8** was heated in THF at 70 °C for 8 h with 4 equiv of cesium hydroxide. Rather than the predicted complex **7**, the μ -hydroxo dinuclear complex $[(\text{NNC}^{t\text{-Bu}})\text{Ir}(\text{Ph})(\mu\text{-OH})_2]$ (**9**) was isolated by recrystallization.

The dinuclear complex was confirmed by synthesis from the previously reported μ -chloro dinuclear complex $[(\text{NNC}^{t\text{-Bu}})\text{Ir}(\text{Ph})(\mu\text{-Cl})_2]$ (**10**).⁴ Heating **10** at 70 °C for 8 h with 4 equiv of cesium hydroxide in THF followed by recrystallization using CH₂Cl₂ and pentane also gave **9**, a black, air-stable solid in 38% yield. Complex **9** was characterized by ¹H and ¹³C NMR, high-resolution mass spectrometry, elemental analysis, and X-ray crystallography (Figure 5).

Since the chloro group could be replaced with a more labile group, such as trifluoroacetate, it might be possible to synthesize **7** under milder conditions. Therefore, the $(\text{NNC}^{t\text{-Bu}})\text{Ir}(\text{Ph})(\text{TFA})\text{Py}$ species **11** was synthesized from **8** using silver trifluoroacetate in CH₂Cl₂. This reaction was sluggish at room temperature, taking approximately 7 days to run to completion. After silver chloride and solvent were removed, **11** was obtained by recrystallization as a reddish orange, air-stable solid in 85% yield. Attempts to synthesize **7** from **11** proved unsuccessful. Reacting **11** in THF-*d*₈ with 4 equiv of cesium hydroxide at room temperature over 2 days produced **9** in 49% yield by proton NMR using internal standardization. These reactions suggest that the ΔG value

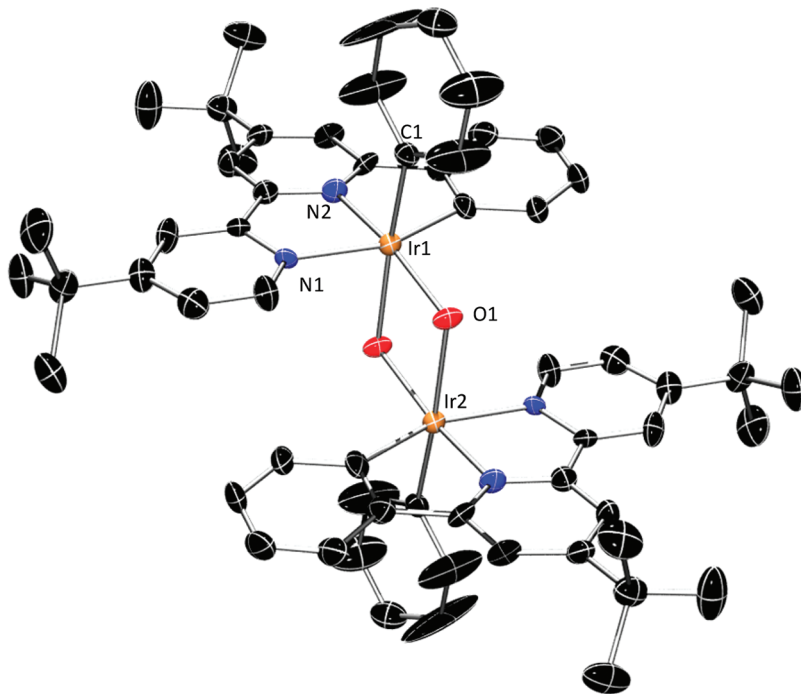
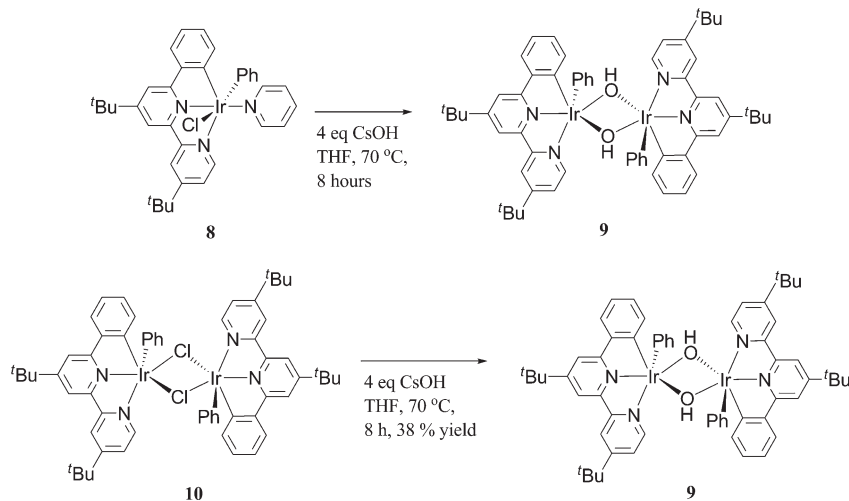


Figure 5. ORTEP diagram of **9**. Thermal ellipsoids are given at the 50% probability level, with hydrogens, a molecule of water, and CH_2Cl_2 omitted for clarity. Selected bond distances (\AA): Ir(1)–O(1), 2.093(8); Ir(1)–C(1), 1.99(14); Ir(1)–N(1), 2.150(9); Ir(1)–N(2), 1.964(10). Selected bond angles (deg): Ir(1)–O(1)–Ir(2), 101.7(3); N(2)–Ir(1)–O(1), 170.7(4).

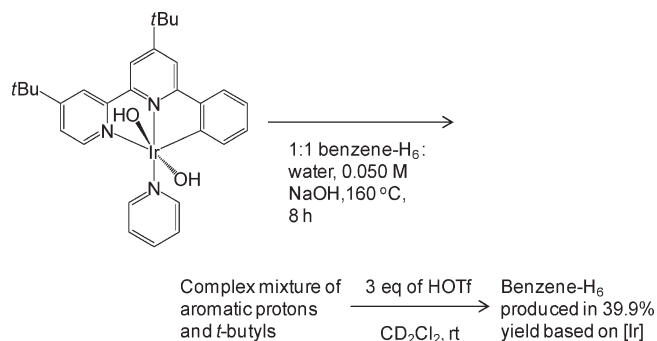
Scheme 2. Synthesis of Possible Phenyl Intermediate



for formation of **9** from **7** is favorable and **9** likely efficiently enters the H/D exchange catalytic cycle. In fact, **9** catalyzes H/D exchange between benzene and water with a TOF of $7.0 \times 10^{-3} \text{ s}^{-1}$ at 190 °C. This TOF is very similar to that observed on starting with **6** (TOF = $6.4 \times 10^{-3} \text{ s}^{-1}$ at 190 °C).

We attempted to directly produce **9** from **6** by carrying out the H/D exchange reaction on a preparative scale. Analysis of the ^1H NMR spectrum of the catalytic reaction did not reveal the presence of **6** or the $\text{NNC}^{t\text{-Bu}}$ ligand, and the presence of **9** is difficult to determine, due to the large number of aromatic peaks from the multiple products produced in the reaction. Attempts to isolate **9** from this mixture failed both by recrystallization and by separation on column chromatographic supports due to the instability of **9** on chromatographic material. However, the furthest downfield

chemical shift in the ^1H NMR of the catalytic reaction is at δ 8.5 ppm. Known mononuclear complexes used as precursors during synthesis have a characteristic chemical shift for the ortho proton on the pyridyl ($\text{NNC}^{t\text{-Bu}}$) ligand that appears at δ 9 ppm or further downfield. The two phenyl dinuclear complexes **9** and **10**, $[(\text{NNC}^{t\text{-Bu}})\text{Ir}(\text{Ph})(\mu\text{-X})_2]$ ($\text{X} = \text{Cl}, \text{OH}$), have their farthest downfield chemical shift no greater than δ 8.5 ppm in the ^1H NMR. This suggests that the product mixture likely contains various dinuclear complexes. Further support for this comes when **6** is heated in a J. Young NMR tube containing H_2O , KOH , and C_6D_6 . Monitoring the NMR reaction over time shows that **6** essentially goes away over the course of 4 h at 160 °C with the formation of free pyridine. The pyridine formation was also confirmed by GC-MS. The formation of free pyridine in the reaction suggests that OH-bridged dinuclear complexes

Scheme 3. Benzene and D₂O H/D Exchange Reaction using 6 under Catalytic Conditions To Detect Phenyl Intermediates


are forming. It should also be pointed out that during the course of the NMR reaction the number of *tert*-butyl groups increases (greater than nine sets of *tert*-butyl groups) over 4 h, indicating that multiple species are formed in the reaction. To determine how much of the products in the preparative-scale reaction contain a phenylated species, trifluoromethanesulfonic acid was reacted with the product mixture (Scheme 3). The resulting protonolysis resulted in free benzene-H₆ and was quantified by using mesitylene as an internal standard. The benzene produced was determined to be 40%, on the basis of the amount of **6** used. Decomposition of the NNC^{*t*-Bu} ligand was not observed in the presence of trifluoromethanesulfonic acid. We attempted to cleave the iridium–phenyl bond of **9** by heating a suspension of **9** in a 0.01 M KOD/D₂O solution at 130–160 °C, but only the starting material **9** was recovered. Higher temperatures resulted in charring of the material.

Density Functional Theory Investigation. To study possible catalytic intermediates and low-energy pathways for benzene H/D exchange, we have employed density functional theory (DFT) calculations. All DFT calculations were performed in Jaguar 7.0 and 7.5.¹⁵ All reactant and transition structures were optimized using B3LYP/LACVP** hybrid-density functional theory. Reported free energies are the sum ΔE (B3LYP/LACV3P++**//B3LYP/LACVP**) + ΔU + pV – 298 ΔS + ΔG (solvation); U and S values were obtained from B3LYP/LACVP** structures. Selected M06/LACV3P++**¹⁶ functional electronic energies evaluated using B3LYP structures are also reported. M06 calculations were run using tight convergence criteria and a very dense grid.¹⁷ Benzene ($\epsilon = 2.284$, radius probe 2.6) and water ($\epsilon = 80.37$, radius probe 1.4) implicit free energy of solvation corrections were applied using the Poisson–Boltzmann solvation model. All transition structure figures were generated using CYL mol.¹⁸ The NNC pincer ligand was modeled without the *tert*-butyl groups, and structure **12** is the model of complex **6**.

Experimentally, when **6** was heated in a solution of D₂O, several new species appeared in the proton NMR spectra. However, addition of 4 equiv of KOD suppressed the generation of these new species. To investigate the role of hydroxide and identify possible species generated in water,

the thermodynamics for solvent–ligand substitution and dinuclear coordination were computed (Scheme 4). The pyridine ligand in structure **12** can rearrange from the meridional position to the apical position in **13**. This isomerization slightly favors structure **13** by –0.3 kcal/mol and is possible if either pyridine or hydroxide dissociates. Pyridine dissociation in water to give structure **14** is endergonic by 13.5 kcal/mol. Water coordination to generate **15** further increases the free energy to 15.5 kcal/mol, while hydroxide coordination to generate the anionic trihydroxo species **16** is slightly favorable from **14** but still endergonic by 10.9 kcal/mol compared to **12**. Outer-sphere explicit water molecules were also used to test whether hydrogen bonding would substantially lower the energies of complexes **14**–**16**. However, the typical energy difference by using a mixed explicit/implicit solvation model was only ~1 kcal/mol.

Although hydroxide dissociation to give the cationic five-coordinate pseudo-trigonal-bipyramidal structure **17** is endergonic by 10.3 kcal/mol, the formation of the dinuclear species **18** from the combination of two hydroxo-pyridine species is exergonic by ~–13 kcal/mol. The M06 functional predicts a slightly more exergonic dinuclear species of –17 kcal/mol. It is possible that substantial hydroxide concentration offsets this equilibrium and prevents formation of **18** and other species.

Without substantial KOD, benzene–D₂O hydrogen–deuterium exchange is also very slow. Although complex **6** is initially soluble in water, the CH activation chemistry was determined experimentally to occur in the benzene phase. Although water and hydroxide have limited solubility in benzene, it is plausible that water or hydroxide may assist or be directly involved in the mechanism of H/D exchange. Therefore, we have extensively explored possible C–H activation transition states with explicit hydroxide and water molecules.

In benzene, B3LYP predicts pyridine dissociation to generate the square-pyramidal five-coordinate intermediate **14** to require 13.1 kcal/mol ($\Delta G_{M06} = 21.1$ kcal/mol). Coordination of benzene via η^2 binding can potentially occur *cis* (**19**) or *trans* (**21**) to the NNC pincer ligand (Scheme 5). However, attempts to optimize structure **21** resulted in a dissociated benzene molecule and **14** due to the labilizing effect of the cyclometalated NNC pincer ligand. *Cis* η^2 binding to give **19** is 29.0 kcal/mol above **14**. From **19**, C–H bond substitution may occur if the hydrogen is transferred to an inner-sphere hydroxo ligand with concomitant Ir–C bond formation. The resulting iridium phenyl species **20** is endergonic by 7.0 kcal/mol, while the alternative ligand arrangement (structure **22**) either generated directly or resulting from water dissociation is significantly more endergonic with a free energy of 19.9 kcal/mol. Although **20** and **22** are endergonic, water loss followed by pyridine recoordination gives the exergonic structures **24** and **25**. Importantly, the dinuclear species **23** (Scheme 5b) formed from the various iridium phenyl species is exergonic. Structures **25** and **23** are predicted to be the lowest energy intermediates upon reaction of **12** with benzene.

A search for possible transition states revealed a viable CH activation route to structure **20** by an internal substitution (IS) transition state (**TS1**, Figure 6).¹⁹ In this

(15) (a) *Jaguar*, version 7.0; Schrodinger, LLC, New York, 2007. (b) *Jaguar*, version 7.5; Schrodinger, LLC, New York, 2009.

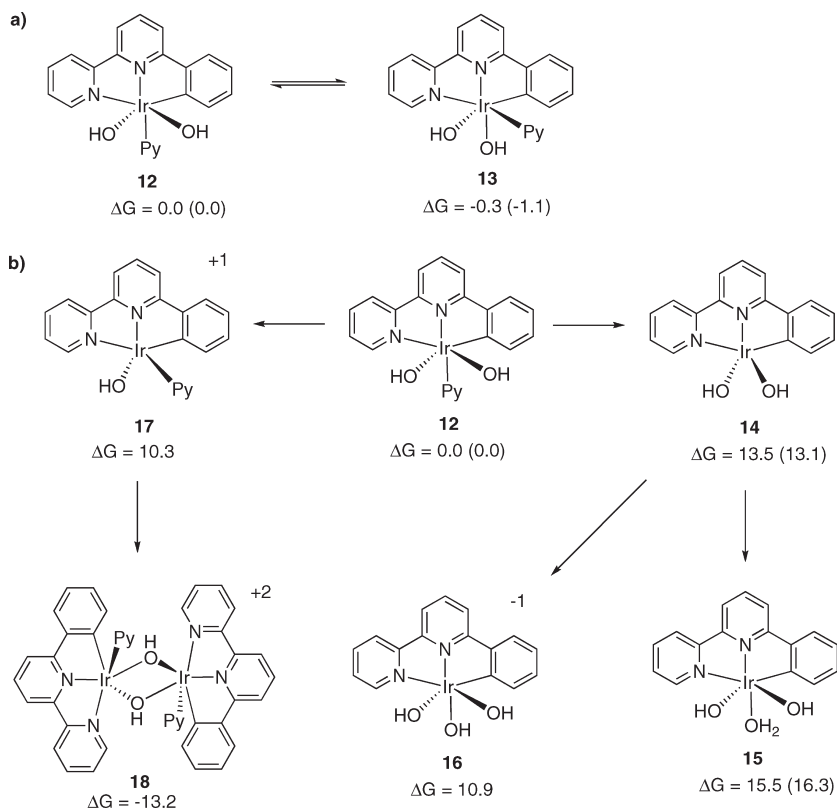
(16) Zhao, Y.; Truhlar, D. G. *Acc. Chem. Res.* **2008**, *41*, 157.

(17) Jaguar options applied: iacc = 1; gdfmed = –14; gdfnfin = –14; gdfngrad = –14.

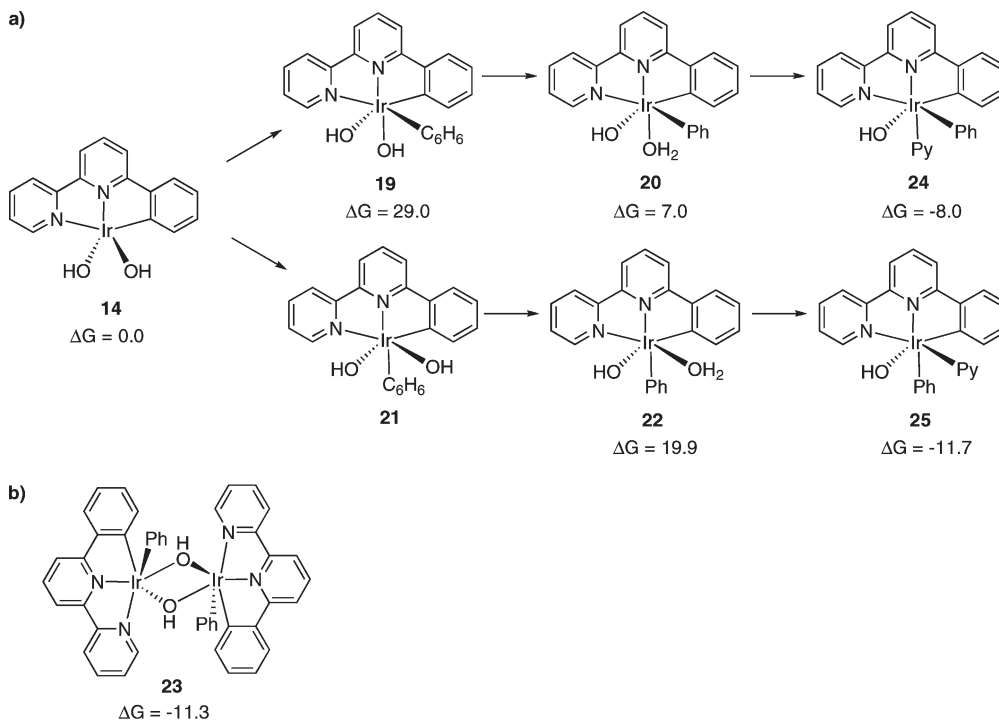
(18) Legault, C. Y. *CYLview*, 1.0b; Université de Sherbrooke, **2009** (<http://www.cylview.org>).

(19) The π -complex **19** is not directly connected to **20**, but rather there is an agostic interaction with the benzene C–H bond.

Scheme 4. Relative free energies in water. Values in parentheses are relative free energies in benzene. (kcal/mol)



Scheme 5. Relative Reaction Free Energies for (a) Benzene CH Activation and (b) Dinuclear Formation



four-membered metathesis-like transition structure, the C–H bond is substantially broken to 1.33 Å and the hydrogen is transferred to the oxygen atom at a distance of 1.34 Å. The newly forming Ir–Ph bond has a distance of 1.32 Å, and the Ir–OH bond is only slightly stretched to

2.14 Å. This IS transition state is similar to the previously reported transition states for the reactions of $(\kappa^2\text{-}O,O\text{-acac})_2\text{Ir}(\text{OH})(\text{pyridine})$ and $(\kappa^2\text{-}O,O\text{-acac})_2\text{Ir}(\text{OMe})(\text{pyridine})$ with benzene.¹³ In **TS1** the benzene hydrogen atom is transferred to the oxygen lone pair while the

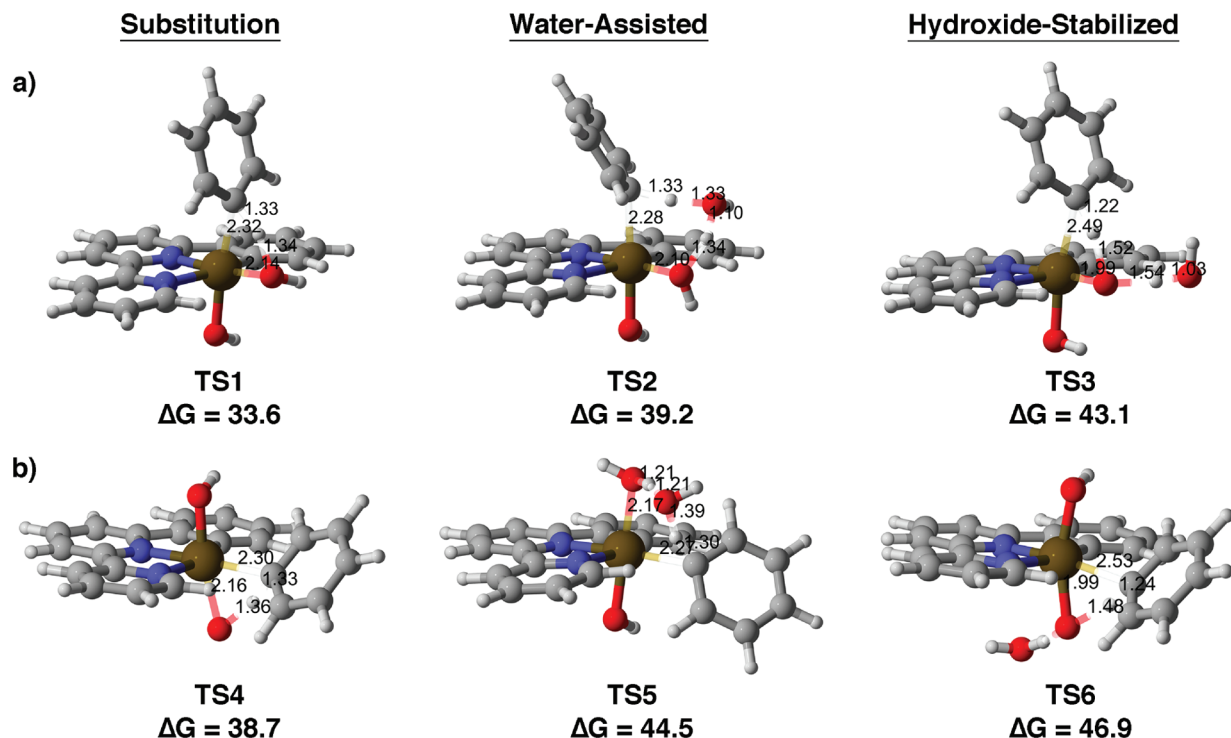


Figure 6. Potential benzene C–H bond activation transition states (a) cis to NNC pincer ligand and (b) trans to NNC pincer ligand.

hydroxo group remains σ -ligated, which is different from a classic σ -bond metathesis mechanism.²⁰ Although the cyclo-metalated NNC pincer ligand is electron donating, the iridium center remains electrophilic with a Mulliken charge of 0.46e to induce Ir–Ph bond formation while the nucleophilic iridium hydroxide fragment abstracts the protic benzene hydrogen. The Mulliken charge on the benzene H atom is 0.37e. The benzene carbon atom and the iridium hydroxide group are both negatively charged in **TS1**: $-0.20e$ and $-0.62e$, respectively. Because of the electrophilic/nucleophilic character of this substitution transition state, the benzene C–H bond is activated by an ambiphilic mechanism.^{20c}

The activation free energy for **TS1** is 33.6 kcal/mol relative to structure **14**; the overall activation free energy from **12** is 46.7 kcal/mol. This is slightly too large to fit with experiment. The M06 functional predicts a more reasonable free energy barrier of 25.4 kcal/mol relative to **14** and 38.5 kcal/mol relative to **12**.²¹ A similar transition state for forming structure **22** via **TS4** was also located but is 5.1 kcal/mol higher due to the trans NNC ligand effect and steric crowding by the NNC ligand, which results in twisting of the incoming phenyl group.

A water molecule may directly assist in CH activation by shuttling a proton from benzene to the hydroxo group. However, these six-membered “water-assisted” transition states, **TS2** and **TS5**, are 5.6 and 10.9 kcal/mol above **TS1**. In combination with the penalty for H₂O to shuttle from water into benzene, estimated as ~ 6 kcal/mol on the basis of

differences in free energies of solvation, it is unlikely that water is directly involved in CH activation in the benzene phase.

No transition states were located for direct deprotonation of benzene by an external hydroxide with concomitant Ir–Ph bond formation. Alternatively, transition states **TS3** and **TS6** were located, which utilize an outer-sphere hydroxide to deprotonate the Ir–OH bond during CH activation. This hydroxide stabilization substantially alters the transition-state geometry compared to **TS1**. **TS3** is earlier along the reaction pathway; the forming Ir–Ph bond is longer (2.49 Å), and the breaking C–H bond is shorter (1.22 Å). This transition state may best be described as the reaction of benzene with an iridium oxide. The Ir–O bond shortens from 2.14 Å in **TS1** to 1.99 Å in **TS3**, and the new hydroxide-hydrogen bond is nearly fully formed at 1.03 Å. However, despite the large effect of the hydroxide on the transition-state geometry, **TS3** and **TS6** are 9.5 and 13.3 kcal/mol above **TS1**. These transition states are even less viable, considering the very poor solubility of hydroxide in benzene and differences in solvation free energy.

As further evidence against water and/or hydroxide direct participation in CH activation, we also considered the energies for **TS1**–**TS3** in water. Relative to structure **14**, the activation free energies are 24.7, 36.6, and 57.6 kcal/mol for **TS1**–**TS3**. This eliminates the possibility of water and hydroxide participation, but **TS1** is 8.9 kcal/mol lower in energy in water than in benzene. The resulting iridium phenyl aquo structure **20** and dinuclear structure **23** are both significantly more exergonic in water: -7.9 and -34.2 kcal/mol relative to **14**. However, as shown by the independent synthesis of **9/23**, this complex is not soluble in water. Although it is beyond the scope of this current investigation, there remains the possibility that CH activation and H/D exchange may occur at the water–benzene interface whereby solubility and solvation effects are optimally balanced.

We have also explored whether the NNC pincer ligand is a spectator ligand or active participant in H/D exchange.

(20) (a) Oxgaard, J.; Tenn, W. J., III; Nielsen, R. J.; Periana, R. A.; Goddard, W. A., III *Organometallics* **2007**, *26*, 1565. (b) Ess, D. H.; Bischof, S. M.; Oxgaard, J.; Periana, R. A.; Goddard, W. A., III *Organometallics* **2008**, *27*, 6440. (c) Ryabov, A. D. *Chem. Rev.* **1990**, *90*, 403. (d) Canty, A. J.; van Koten, G. *Acc. Chem. Res.* **1995**, *28*, 406. (e) Ess, D. H.; Nielsen, R. J.; Goddard, W. A., III; Periana, R. A. *J. Am. Chem. Soc.* **2009**, *131*, 11686.

(21) MPW1K/LACV3P++** predicts a free energy barrier of 25.5 kcal/mol, similar to that for M06.

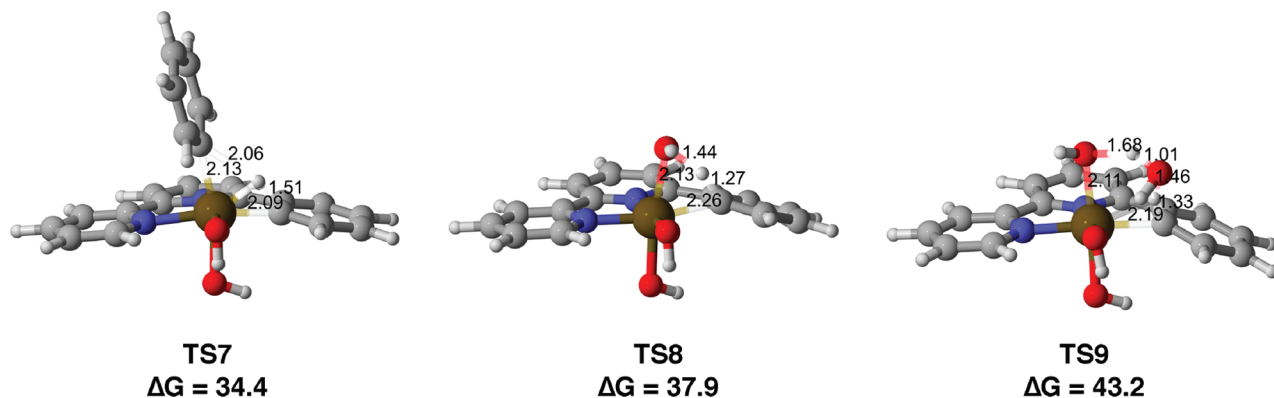
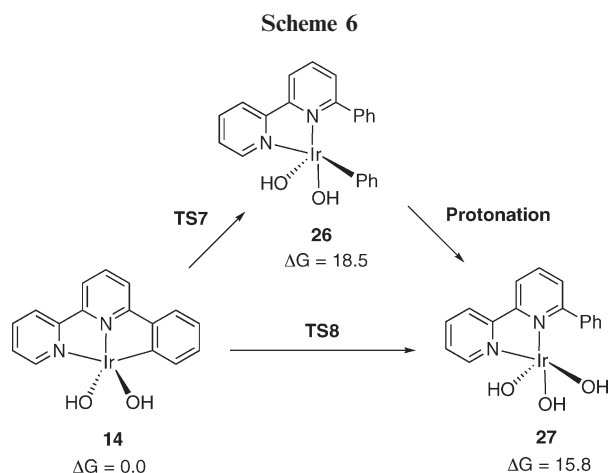


Figure 7. Proton transfer transition states to the NNC ligand.



Addition of the benzene C–H bond across the cyclometalated Ir–C bond would give the iridium phenyl species **26** (Scheme 6). No oxidative Ir(V) hydride intermediate was located between **14** and **26**. The transition state, **TS7**, is similar to other so-called “oxidative hydrogen migration” (OHM) transition states where there is significant oxidative character but no intermediate.²² In this metal-assisted σ bond metathesis transition state the newly forming Ir–Ph bond and breaking Ir–C bond lengths are very similar: 2.13 and 2.09 Å, respectively. However, the hydrogen atom is not equally shared, due to the constraints imposed by the NNC ligand bonding. The breaking C–H bond is significantly more broken (2.06 Å) and the forming bond C–H bond is much shorter (1.51 Å). The OHM transition state **TS7** (see Scheme 6 and Figure 7) is only 0.8 kcal/mol above **TS1**. Neither water nor hydroxide assistance lowers the energy of **TS7**. From **26**, one pathway whereby H/D exchange may occur is by coordination of D₂O to the vacant site followed by intramolecular protonation to generate the trihydroxo species **27**. Water coordination to **26** is favorable by 10.0 kcal/mol. However, the free energy barrier for phenyl protonation of **26** to **27** is 19.4 and

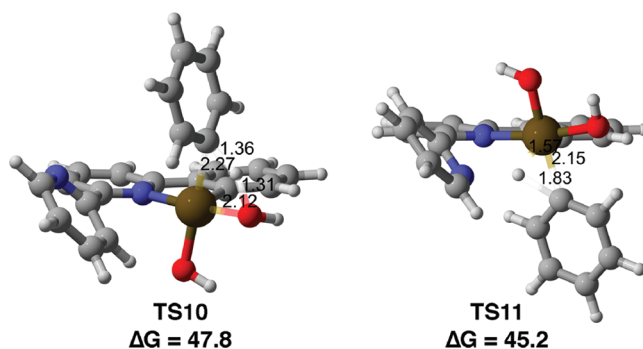


Figure 8. Benzene substitution and oxidative addition transition states with NNC pyridine ligand dissociation.

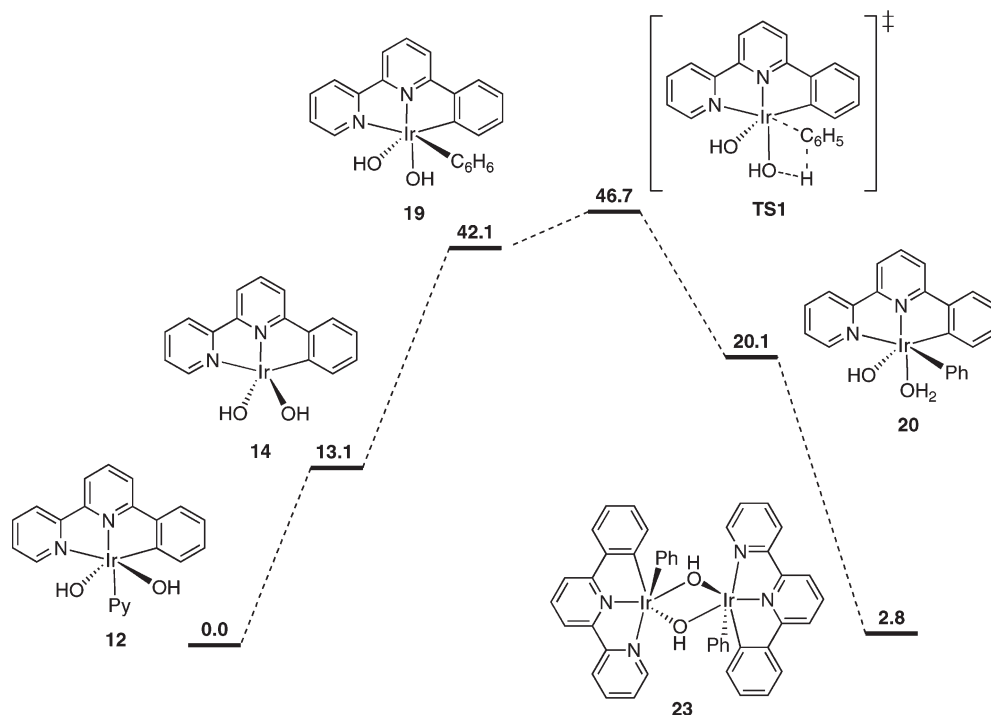
37.9 kcal/mol relative to **14**, making this pathway 4.3 kcal/mol higher than the pathway utilizing **TS1**. The direct route to **27** via **TS8** or **TS9** (Figure 7) requires 3.5 and 8.8 kcal/mol more free energy than **TS7**.

An important issue to explore is the influence and necessity of the pincer-coordinated cyclometalated NNC ligand for CH activation. It is possible that the pyridine portion of the NNC ligand could decoordinate from the iridium center to generate a more electrophilic metal center. In the ground state, pyridine dissociation requires 11–14 kcal/mol of free energy. The corresponding transition state, **TS10** (Figure 8), has an activation free energy of 47.8 kcal/mol. This is 14.2 kcal/mol above the fully coordinated transition state **TS1**, showing that there is no beneficial transition state effect for pyridine to decoordinate, and so it prefers to remain ligated during CH activation. It is also conceivable that pyridine decoordination would open two cis sites to allow for oxidative addition to an Ir(V) hydride species. Although this transition state, **TS11** ($\Delta G^\ddagger = 45.2$ kcal/mol), is lower in energy than **TS10**, where no formal oxidation takes place, it is still too high to be competitive with **TS1**.

On the basis of the activation free energies for all of the transition states explored, catalytic H/D exchange between benzene and water likely occurs via an internal substitution pathway, as outlined in Scheme 7. With significant hydroxide concentration, the starting structure **12** will not convert into the lower energy dinuclear species **18**. From **12**, the π -complex **19** is generated via pyridine loss and benzene coordination. Rearrangement to interaction with the C–H bond followed by cleavage with a hydroxo group gives the iridium phenyl species **20**. Water–D₂O exchange may occur at this point and then undergo the microscopic reverse of CH

(22) (a) Oxgaard, J.; Muller, R. P.; Goddard, W. A., III; Periana, R. A. *J. Am. Chem. Soc.* **2004**, *126*, 352. (b) Webster, C. E.; Fan, Y.; Hall, M. B.; Kunz, D.; Hartwig, J. F. *J. Am. Chem. Soc.* **2003**, *125*, 858. (c) Hartwig, J. F.; Cook, K. S.; Hapke, M.; Incarvito, C. D.; Fan, Y.; Webster, C. E.; Hall, M. B. *J. Am. Chem. Soc.* **2005**, *127*, 2538. (d) Ng, S. M.; Lam, W. H.; Mak, C. C.; Tsang, C. W.; Jia, G.; Lin, Z.; Lau, C. P. *Organometallics* **2003**, *22*, 641. (e) Lam, W. H.; Jia, G.; Lin, Z.; Lau, C. P.; Eisenstein, O. *Chem. Eur. J.* **2003**, *9*, 2775. (f) In these references OHM transition states have been referred to as metal-assisted σ -bond metathesis, oxidatively added transition state, and σ -complex assisted metathesis. For a recent review see: Perutz, R. N.; Sabo-Etienne, S. *Angew. Chem., Int. Ed.* **2007**, *46*, 2578.

Scheme 7. Free Energy Profile for IS Catalytic H/D Exchange



activation. After water loss and prior to D₂O coordination it is also likely that the dinuclear structure **23** is formed in a reversible process. Structures **12** and **23** are nearly equal in free energy, and therefore, formation of this dinuclear species does not increase the free energy span for H/D exchange.

Conclusion

In summary, we have reported the synthesis of a water-soluble cyclometalated dihydroxo iridium(III) pyridyl complex, **6**. This complex is capable of H/D exchange between water and benzene in the presence of base. Experimental and density functional studies suggest that H/D exchange occurs through disassociation of pyridine to generate a *cis*-dihydroxo complex, which then heterolytically activates the benzene C-H bond by an ambiphilic substitution transition state.

Experimental Section

General Considerations. Unless otherwise noted, all reactions were performed using standard Schlenk techniques (argon) or in a MBraun glovebox (nitrogen). GC-MS analyses were performed on a Shimadzu GC-MS QP5000 instrument (version 2) equipped with a cross-linked methyl silicone gum capillary column (DB5). ¹H and ¹³C NMR spectra were collected on a Varian 400 Mercury Plus spectrometer and referenced to residual protiated solvent. Fluorine resonances were referenced to CFCl₃ or hexafluorobenzene. All coupling constants are reported in hertz (Hz). Mass spectrometry analyses were performed at the UC Riverside mass spectrometry lab. Elemental analyses were performed by Desert Analytical Laboratory, Inc., Tucson, AZ. X-ray crystallographic data were collected on a Bruker SMART APEX CCD diffractometer.

Materials. Trifluoroacetic acid (99%, Aldrich), cesium hydroxide (99%, Aldrich), sodium methoxide (95%, Aldrich), and Drisolv pyridine (99.8%, EMD) were all used as received. All solvents were reagent grade or better. Tetrahydrofuran and

benzene were dried over sodium/benzophenone and distilled under argon. Dichloromethane (stabilizer removed with sulfuric acid) was dried over P₂O₅ and distilled under argon. Complexes **1**, **8**, and **10** were prepared according to the literature.⁴ Chromatotron (centrifugal thin-layer chromatography) plates were made using aluminum oxide neutral (type E) that was purchased from EMD.

Preparation of (NNC^{t-Bu})Ir(Et)(TFA)NCCH₃ (2**).** Under an inert atmosphere, CH₂Cl₂ (30 mL) was added to a Schlenk flask containing **1** (620.4 mg, 0.9674 mmol) and silver trifluoroacetate (235.0 mg, 1.064 mmol). The mixture was stirred in the dark for 2 days, followed by filtration over Celite to remove the silver chloride. The solvent was removed under reduced pressure, and the product was obtained by recrystallization from CH₂Cl₂ and pentane at -30 °C, resulting in a 78.2% (543.8 mg) yield. ¹H NMR (CDCl₃, 400 MHz): δ 8.87 (d, 1H, ³J = 6.0 Hz), 7.85 (d, 1H, ⁴J = 1.6 Hz), 7.63 (d, 1H, ⁴J = 1.4 Hz), 7.58 (d, 1H, ⁴J = 1.4 Hz), 7.53 (d, 1H, ³J = 7.4 Hz), 7.50 (d, 1H, ³J = 8.0 Hz), 7.46 (dd, 1H, ³J = 6.0 Hz, ⁴J = 1.9 Hz), 7.14 (t, 1H, ³J = 7.3 Hz), 6.99 (t, 1H, ³J = 7.0 Hz), 2.58 (s, 3H, -NCCH₃), 1.44 (s, 9H), 1.42 (s, 9H), 0.87 (m, 1H, Ir-CH₂CH₃), 0.58 (m, 1H, Ir-CH₂CH₃), 0.09 (t, 3H, -CH₂CH₃, ³J = 7.9 Hz). ¹³C{¹H} NMR (CDCl₃, 100 MHz): δ 168.4, 162.3, 162.2 (O₂CCF₃, ²J_{C-F} = 35.4 Hz), 161.5, 158.0, 156.6, 152.8, 151.0, 146.0, 134.0, 130.8, 124.7, 123.8, 121.1, 118.7, 116.4, 116.31 (COCF₃, ¹J_{C-F} = 294 Hz), 114.7, 113.9, 35.51, 35.49, 31.07, 30.73, 16.6, 4.62, -15.42. ¹⁹F NMR (CD₂Cl₂, 376 MHz): δ -74.79 (s, 3F). High-resolution ESI for C₃₀H₃₅N₃O₂F₃Ir: calcd mass [M - TFA]⁺ *m/z* 606.2460; found *m/z* 606.2400.

Preparation of (NNC^{t-Bu})Ir(TFA)₂NCCH₃ (3**).** Under an inert atmosphere, complex **2** (1.644 g, 2.289 mmol) was stirred overnight with trifluoroacetic acid (60 mL) in a Schlenk flask. The solvent was removed under reduced pressure, and the resulting brown, oily residue was redissolved in CH₂Cl₂. Compound **3** was purified using column chromatography (basic alumina), and it was eluted as a yellow band with 95% CH₂Cl₂/5% ethyl acetate in a 60.2% (1.103 g) yield. ¹H NMR (CD₂Cl₂, 400 MHz): δ 9.32 (d, 1H, ³J = 5.8 Hz), 8.08 (d, 1H, ⁴J = 1.8 Hz), 7.88 (d, 1H, ⁴J = 1.5 Hz), 7.85 (d, 1H, ⁴J = 1.5 Hz), 7.72 (m, 3H), 7.32 (dt, 1H, ³J = 7.7 Hz, ⁴J = 1.4 Hz), 7.17 (dt, 1H, ³J = 7.6 Hz,

$^4J = 1.1$ Hz), 2.81 (s, 3H), 1.55 (s, 9H), 1.51 (s, 9H). $^{13}\text{C}\{^1\text{H}\}$ NMR (CD_2Cl_2 , 100 MHz): δ 168.5, 165.1, 164.6, 164.1 ($\text{CO}(\text{CF}_3)$), $^2J_{\text{C-F}} = 35.7$ Hz), 158.1, 157.6, 153.6, 147.3, 141.3, 135.8, 130.9, 125.2, 124.1, 123.9, 119.8, 118.8, 115.9, 115.6, 112.6 ($\text{CO}(\text{CF}_3)$), $J_{\text{C-F}} = 290.7$ Hz), 36.0 ($-\text{C}(\text{CH}_3)_3$), 35.9 ($-\text{C}(\text{CH}_3)_3$), 31.1 ($-\text{C}(\text{CH}_3)_3$), 30.8 ($-\text{C}(\text{CH}_3)_3$), 4.5 ($\text{Ir}-\text{NCCH}_3$). ^{19}F NMR (CD_2Cl_2 , 376 MHz): δ -75.09 (s, 3F). Anal. Calcd for $\text{C}_{30}\text{H}_{30}\text{N}_3\text{O}_4\text{F}_6\text{Ir}$: C, 44.88; H, 3.77; N, 5.23; F, 14.20. Found: C, 44.96; H, 3.79; N, 5.16; F, 14.63. High-resolution FAB $^+$ (^{191}Ir) for $\text{C}_{30}\text{H}_{30}\text{N}_3\text{O}_4\text{F}_6\text{Ir}$: calcd mass m/z [M] $^+$ 801.1746, found m/z 801.1717.

Preparation of $(\text{NNC}^t\text{-Bu})\text{Ir}(\text{TFA})_2\text{Py}$ (4). Complex **3** (1.103 g, 1.374 mmol) was dissolved in degassed pyridine (40 mL). The solution was heated overnight in a Schlenk bomb at 100 °C. The pyridine was removed under reduced pressure to give an orange solid, which was redissolved in CH_2Cl_2 . Complex **4** was purified by column chromatography (basic alumina), and it was eluted from the column as an orange band with an eluent mixture of 25% pentane and 75% CH_2Cl_2 in a 94.2% (1.088 g) yield. ^1H NMR (CD_2Cl_2 , 400 MHz): δ 9.09 (dd, 2H, $^3J = 5.3$ Hz, $^4J = 1.5$ Hz), 8.53 (d, 1H, $^3J = 5.5$ Hz), 8.20 (d, 1H, $^4J = 1.8$ Hz), 8.08 (dt, 1H, $^3J = 7.6$ Hz, $^4J = 1.6$ Hz), 7.96 (d, 2H), 7.79 (dd, 1H, $^3J = 7.8$ Hz, $^4J = 1.6$ Hz), 7.66 (m, 3H), 7.22 (dt, 1H, $^3J = 7.6$ Hz, $^4J = 1.8$ Hz), 7.15 (dt, 1H, $^3J = 7.6$ Hz, $^4J = 1.5$ Hz), 6.96 (dd, 1H, $^3J = 7.6$ Hz, $^4J = 1.2$ Hz), 1.62 (s, 9H, *t*-Bu), 1.53 (s, 9H, *t*-Bu). $^{13}\text{C}\{^1\text{H}\}$ NMR (CD_2Cl_2 , 100 MHz): δ 168.6, 164.5, 164.4, 163.6 ($\text{O}_2\text{C}(\text{CF}_3)$), $^2J_{\text{C-F}} = 36.6$ Hz), 160.0, 158.2, 155.0, 152.1, 150.1, 149.0, 141.5, 138.3, 133.6, 130.3, 126.3, 124.9, 124.0, 123.7, 119.7, 115.5, 115.1, 112.7 ($\text{O}_2\text{C}(\text{CF}_3)$), $J_{\text{C-F}} = 291.3$ Hz), 35.93 ($-\text{C}(\text{CH}_3)_3$), 35.90 ($-\text{C}(\text{CH}_3)_3$), 31.3 ($-\text{C}(\text{CH}_3)_3$), 30.8 ($-\text{C}(\text{CH}_3)_3$). ^{19}F NMR (CD_2Cl_2 , 376 MHz): δ -75.63 (s, 3F). Anal. Calcd for $\text{C}_{33}\text{H}_{32}\text{N}_3\text{O}_4\text{F}_6\text{Ir}$: C, 47.14; H, 3.84; N, 5.00; F, 13.56. Found: C, 46.73; H, 3.71; N, 4.83; F, 13.53. High-resolution FAB $^+$ (^{191}Ir) for $\text{C}_{33}\text{H}_{32}\text{N}_3\text{O}_4\text{F}_6\text{Ir}$: calcd mass [M] $^+$ m/z 839.1903, found m/z 839.1878.

Preparation of $(\text{NNC}^t\text{-Bu})\text{Ir}(\text{OMe})_2\text{Py}$ (5). Under an inert atmosphere, **4** (313.3 mg, 0.3726 mmol) and sodium methoxide (330.7 mg, 6.122 mmol) were dissolved in methanol (30 mL) in a Schlenk bomb. The bomb was sealed and heated at 70 °C for 24 h. The solvent was removed under reduced pressure, and the resulting solid was dissolved in CH_2Cl_2 . The solution was filtered over Celite to remove the excess sodium methoxide. The process of filtering out the excess sodium methoxide was repeated until the solution could easily be filtered through a pipet plug of Celite. Complex **5** was purified by centrifugal thin-layer chromatography (Chromatotron) using a neutral alumina Chromatotron plate. The product was eluted as a blackish green band with 4% methanol/96% ethyl acetate as the eluent to yield a black solid in 35.2% (88.2 mg) yield. ^1H NMR (CDCl_3 , 400 MHz): δ 9.52 (dd, 2H, $^3J = 7.0$ Hz, $^4J = 1.4$ Hz), 8.27 (d, 1H, $^3J = 5.8$ Hz), 8.01 (d, 1H, $^4J = 1.8$ Hz), 7.96 (dt, 1H, $^3J = 7.8$ Hz, $^4J = 1.4$ Hz), 7.80 (dd, 2H, $^3J = 6.4$ Hz, $^4J = 1.8$ Hz), 7.63 (m, 1H), 7.58 (dt, 2H, $^3J = 6.2$ Hz, $^4J = 1.4$ Hz), 7.49 (dd, 1H, $^3J = 6.0$ Hz, $^4J = 1.8$ Hz), 7.05 (m, 3H), 2.52 (s, 6H, $\text{Ir}-\text{OCH}_3$), 1.55 (s, 9H), 1.44 (s, 9H). $^{13}\text{C}\{^1\text{H}\}$ NMR (CDCl_3 , 100 MHz): δ 168.5, 162.6, 162.2, 158.1, 156.2, 151.4, 148.5, 146.5, 136.4, 132.4, 130.3, 125.7, 125.2, 125.0, 123.9, 121.6, 119.5, 114.5, 58.9 ($-\text{OMe}$), 35.3 ($-\text{C}(\text{CH}_3)_3$), 35.2 ($-\text{C}(\text{CH}_3)_3$), 31.1 ($-\text{C}(\text{CH}_3)_3$), 30.6 ($-\text{C}(\text{CH}_3)_3$). Anal. Calcd for $\text{C}_{31}\text{H}_{38}\text{N}_3\text{O}_2\text{Ir}$: C, 55.01; H, 5.66; N, 6.21. Found: C, 55.31; H, 6.01; N, 5.93. High-resolution FAB $^+$ (^{191}Ir) for $\text{C}_{31}\text{H}_{38}\text{N}_3\text{O}_2\text{Ir}$: calcd mass [M] $^+$ m/z 675.2570, found m/z 675.2594.

Preparation of $(\text{NNC}^t\text{-Bu})\text{Ir}(\text{OH})_2\text{Py}$ (6). Under an inert atmosphere, **5** (342.2 mg, 0.5055 mmol) was dissolved in a 1:1 (24 mL total volume) mixture of THF and water in a Schlenk bomb. The bomb was sealed and heated at 85 °C for 2 days. Pyridine (15 mL) was added to the reaction mixture to break up the viscosity of the solvent, and the solvent was removed under reduced pressure at 60 °C. The resulting reddish black solid was then dissolved in CH_2Cl_2 and purified by centrifugal thin-layer

chromatography (Chromatotron) using a neutral alumina Chromatotron plate. Complex **6** was eluted as a red band by a slow gradient elution starting with 2% methanol/98% ethyl acetate and increasing the eluent mixture up to 20% methanol/80% ethyl acetate. Complex **5** was obtained as a blackish green solid in 21.4% (70.2 mg) yield. ^1H NMR (CDCl_3 , 400 MHz): δ 9.57 (d, 2H, $^3J = 5.2$ Hz), 8.28 (d, 1H, $^3J = 5.8$ Hz), 7.95 (d, 1H, $^3J = 1.7$ Hz), 7.88 (dt, 1H, $^3J = 7.6$ Hz, $^4J = 1.8$ Hz), 7.72 (d, 1H, $^4J = 1.7$ Hz), 7.71 (d, 1H, $^4J = 1.5$ Hz), 7.57 (dd, 1H, $^3J = 7.6$ Hz, $^4J = 1.4$ Hz), 7.49 (dt, 2H, $^3J = 6.9$ Hz, $^4J = 1.5$ Hz), 7.42 (dd, 1H, $^3J = 5.8$ Hz, $^4J = 1.9$ Hz), 7.01 (dt, 1H, $^3J = 7.2$ Hz, $^4J = 1.5$ Hz), 6.96 (dt, 1H, $^3J = 7.3$ Hz, $^4J = 1.6$ Hz), 6.85 (dd, 1H, $^3J = 7.0$ Hz, $^4J = 1.1$ Hz), 1.47 (s, 9H), 1.36 (s, 9H), -2.71 (bs, 2H, -OH). $^{13}\text{C}\{^1\text{H}\}$ NMR (CDCl_3 , 100 MHz): δ 168.7, 162.4, 161.6, 158.4, 157.1, 151.3, 150.3, 148.9, 147.9, 136.0, 133.3, 130.5, 125.2, 124.8, 124.00, 121.9, 119.4, 114.7, 114.1, 35.3 ($-\text{C}(\text{CH}_3)_3$), 35.2 ($-\text{C}(\text{CH}_3)_3$), 31.3 ($-\text{C}(\text{CH}_3)_3$), 30.8 ($-\text{C}(\text{CH}_3)_3$). Anal. Calcd for $\text{C}_{29}\text{H}_{34}\text{N}_3\text{O}_2\text{Ir}$: C, 53.68; H, 5.28; N, 6.48. Found: C, 53.12; H, 5.19; N, 6.32. High-resolution FAB $^+$ (^{191}Ir) for $\text{C}_{29}\text{H}_{34}\text{N}_3\text{O}_2\text{Ir}$: calcd. mass [M] $^+$ m/z 647.2257, found m/z 647.2265.

Preparation of $[(\text{NNC}^t\text{-Bu})\text{Ir}(\text{Ph})(\mu\text{-OH})_2]$ (9). In a Schlenk bomb, degassed THF (30 mL) was added to a mixture of **10** (150.3 mg, 0.116 mmol) and cesium hydroxide (80.5 mg, 0.479 mmol). The bomb was sealed under argon and heated at 70 °C for 8 h. The solution was filtered over Celite to remove the cesium chloride and excess cesium hydroxide. The Celite was washed with CH_2Cl_2 to dissolve any precipitated **9**. The filtrate was then evaporated to dryness. Complex **9** was obtained in 38% yield (55.2 mg, 0.0436 mmol) as a black solid by recrystallization from CH_2Cl_2 and pentane at -30 °C. ^1H NMR (CDCl_3 , 400 MHz): δ 8.27 (d, 1H, $^3J = 5.8$ Hz), 7.88 (d, 1H, $^4J = 1.5$ Hz), 7.73 (d, 1H, $^4J = 1.3$ Hz), 7.69 (d, 1H, $^3J = 7.7$ Hz), 7.65 (d, 1H, $^3J = 1.5$ Hz), 7.26 (dd, 1H, $^3J = 5.6$ Hz, $^4J = 1.8$ Hz), 7.03 (dt, 1H, $^3J = 7.3$ Hz, $^4J = 1.5$ Hz), 6.75 (dt, 1H, $^3J = 6.7$ Hz), 6.73 (t, 1H, $^3J = 7.3$ Hz), 6.35 (m, 3H), 6.28 (dd, 1H, $^3J = 3.7$ Hz, $^4J = 2.0$ Hz), 1.52 (s, 9H), 1.46 (s, 9H). $^{13}\text{C}\{^1\text{H}\}$ NMR (CDCl_3 , 100 MHz): δ 169.8, 161.1, 158.4, 158.1, 157.4, 156.8, 151.5, 147.7, 135.9, 133.7, 130.0, 129.8, 124.9, 124.4, 123.8, 120.2, 117.9, 114.0, 113.9, 35.3 ($-\text{C}(\text{CH}_3)_3$), 35.2 ($-\text{C}(\text{CH}_3)_3$), 31.2 ($-\text{C}(\text{CH}_3)_3$), 30.8 ($-\text{C}(\text{CH}_3)_3$). Anal. Calcd for $\text{C}_{60}\text{H}_{66}\text{N}_4\text{O}_2\text{Ir}_2$: C, 57.21; H, 5.28; N, 4.45. Found: C, 55.64; H, 5.37; N, 4.41. High-resolution FAB $^+$ (^{191}Ir) for $\text{C}_{60}\text{H}_{66}\text{N}_4\text{O}_2\text{Ir}_2$: calcd mass [M + H] $^+$ m/z 1261.4517, found m/z 1261.4537.

Preparation of $(\text{NNC}^t\text{-Bu})\text{Ir}(\text{Ph})(\text{TFA})\text{Py}$ (11). Under an inert atmosphere, CH_2Cl_2 (30 mL) was added to a Schlenk bomb containing **8** (213.0 mg, 0.2928 mmol) and silver trifluoroacetate (101.8 mg, 0.4610 mmol). The reaction mixture was protected from light with aluminum foil and stirred for 1 week. The solvent was removed under reduced pressure, and the mixture was redissolved in CH_2Cl_2 . The mixture was filtered over Celite to remove the silver chloride. The filtrate was evaporated under reduced pressure to give **11** (200.2 mg, 0.2488 mmol) as an orange solid in 85.2% yield. ^1H NMR (CD_2Cl_2 , 400 MHz): δ 8.99 (d, 1H, $^3J = 5.6$ Hz), 8.06 (m, 4H), 7.87 (d, 1H, $^4J = 1.8$ Hz), 7.83 (dd, 1H, $^3J = 7.4$ Hz, $^4J = 1.1$ Hz), 7.79 (dd, 1H, $^3J = 5.8$ Hz, $^4J = 1.6$ Hz), 7.71 (d, 1H, $^4J = 1.6$ Hz), 7.66 (dt, 1H, $^3J = 7.3$ Hz, $^4J = 1.4$ Hz), 7.36 (dt, 1H, $^3J = 7.5$ Hz, $^4J = 1.4$ Hz), 7.28 (dt, 1H, $^3J = 7.0$ Hz, $^4J = 1.4$ Hz), 7.15 (t, 2H, $^3J = 6.0$ Hz), 6.93 (t, 2H, $^3J = 7.0$ Hz), 6.89 (t, 2H, $^3J = 7.0$ Hz), 6.84 (dt, 1H, $^3J = 7.0$ Hz, $^4J = 1.6$ Hz), 1.50 (s, 9H), 1.38 (s, 9H). $^{13}\text{C}\{^1\text{H}\}$ NMR (CD_2Cl_2 , 100 MHz): δ 167.0, 164.5, 164.3 ($-\text{O}_2\text{CCF}_3$), $^2J_{\text{C-F}} = 35$ Hz), 163.4, 156.4, 155.7, 149.0, 148.1, 147.8, 144.4, 137.9, 132.2, 131.6, 130.5, 127.2, 127.0, 126.6, 125.5, 123.0, 121.6, 120.3, 117.3, 116.6, 115.3, 114.5 ($-\text{O}_2\text{CCF}_3$), $^1J_{\text{C-F}} = 287$ Hz), 35.6 ($-\text{C}(\text{CH}_3)_3$), 35.5 ($-\text{C}(\text{CH}_3)_3$), 30.4 ($-\text{C}(\text{CH}_3)_3$), 30.3 ($-\text{C}(\text{CH}_3)_3$). ^{19}F NMR (CD_2Cl_2 , 376 MHz): δ -75.10 (s, 3F). High-resolution ESI/APCI MS for $\text{C}_{37}\text{H}_{37}\text{N}_3\text{O}_2\text{F}_3\text{Ir}$: calcd mass [M - Ph] $^+$ m/z 728.2076, found m/z 728.2078.

Stability Tests of 6 in D₂O. In three separate J. Young NMR tubes, a 5.0 mM solution of **6** in D₂O was added. To one NMR tube was added 2 equiv of pyridine, and to another NMR tube was added 4 equiv of KOD. The tubes were all heated simultaneously and then analyzed by ¹H NMR. The ¹H NMR study for **6** in neat D₂O and in the presence of 4 equiv of KOD can be found in the Supporting Information.

General Procedure for H/D Exchange Studies of Water/Benzene by 6. In a typical reaction, 0.50 mL of a 3.54 mM solution of **6** in D₂O, 14 equiv of KOD, and 0.50 mL of benzene-H₆ were loaded into a resealable Schlenk tube under argon. The tube was then heated anywhere from 2 to 24 h, depending on the temperature used. After the desired heating, the Schlenk tube was removed from the oil bath, and the benzene layer was analyzed by GC-MS to determine the amount of deuterium incorporation into benzene. To determine if **6** was stable under catalytic conditions, the Schlenk tube was opened under argon and a 0.6 μL aliquot of the benzene layer was analyzed by GC-MS. The Schlenk tube was then resealed and heated for a longer time. This process was repeated several times to ensure that a plot of TON vs time was linear (see the Supporting Information).

Analysis of H/D Exchange. Catalytic H/D exchange reactions were quantified by monitoring the increase of deuterium into C₆H₆ by GC-MS analyses. This was achieved by deconvoluting the mass fragmentation pattern obtained from the MS analysis, using a program developed with Microsoft EXCEL.²³ An important assumption made with this method is that there are no isotope effects on the fragmentation pattern for the various benzene isotopologues. Fortunately, because the parent ion of benzene is relatively stable toward fragmentation, it can be used reliably to quantify the exchange reactions. The mass range from *m/z* 78 to 84 (for benzene) was examined for each reaction and compared to a control reaction where no metal catalyst was added. The program was calibrated with known mixtures of benzene isotopologues. The results obtained by this method are reliable to within 5%. Thus, analysis of a mixture of C₆H₆, C₆D₆, and C₆H₅D prepared in a molar ratio of 50.6:25.3:24.1 resulted in an experimentally determined ratio of 49.4 (C₆H₆):23.3 (C₆D₆):27.3 (C₆H₅D₁). Catalytic H/D exchange reactions were thus run for sufficient reaction times to be able to detect changes to >5% exchange. H/D exchange reactions of benzene were carried out such that less than 10% deuterium incorporation had occurred. This allowed for the kinetics to remain pseudo first order. Keeping the deuterium incorporation to a small amount also prevented the statistical chance that degenerate deuterium/deuterium exchange would occur.

Background Analysis. To ensure that catalysis was occurring, control reactions were conducted to account for the amount of H/D exchange observed from a reaction mixture containing D₂O, KOD, and benzene-H₆. The reaction conditions were conducted similarly to those described in General Procedure for H/D Exchange Studies of Water/Benzene by **6**. However, the solution contained no added catalyst. These solutions were

analyzed as described above. Results of the control (background) and the catalytic reaction can be seen in Table 1.

Catalyst Phase Removal. Under an inert atmosphere, **9** (8.9 mg, 7.0 mmol), KOD (0.10 mmol, 14 equiv), benzene-H₆ (2.0 mL), and D₂O (2.0 mL) were added in a Schlenk bomb. The bomb was sealed and heated in an oil bath at 190 °C for 17 h, after which the reaction was cooled to room temperature. The benzene phase was completely removed and analyzed by GC-MS, resulting in a TOF of $7.5 \times 10^{-3} \text{ s}^{-1}$ (23.2% C₆H₅D and 2.8% C₆H₄D₂) with the results corrected for background H/D exchange. Degassed benzene-H₆ containing no catalyst was added to the remaining aqueous solution in the Schlenk bomb. The bomb was sealed and heated at 190 °C for another 17 h. Analysis of the benzene phase showed little to no H/D exchange (less than 0.5% benzene-H₆ converted, which is within analytical error of the GC-MS).

Mass Transfer Study. Using the procedure described in General Procedure for H/D Exchange Studies of Water/Benzene by **6**, separate Schlenk tubes were analyzed under different stirring rates at the highest temperature that would be used in these studies, 190 °C. The turnover frequencies observed at the various stirring rates were within error ($\pm 1.0 \times 10^{-3} \text{ s}^{-1}$) of what might be expected at 190 °C.

Preparative-Scale Attempt To Produce 9 from 6. Under argon, 6 mL of a 2.12 mM stock solution of **6** (0.0127 mmol) in H₂O and 6 mL of benzene-H₆ were added to a resealable Schlenk tube. Aqueous sodium hydroxide was added to make the aqueous phase a 0.050 M NaOH (aqueous) solution. The Schlenk bomb was sealed and heated at 160 °C for 8 h. The reaction mixture was cooled to room temperature, and 3 mL of pyridine was added to the mixture. The tube was sealed and heated at 50 °C for 1 h prior to removal of the solvent from the mixture under reduced pressure with gentle heating. The mixture was redissolved in CD₂Cl₂ and checked to ensure that there was no observable benzene-H₆ by ¹H NMR. Trifluoromethanesulfonic acid (5 μL) was added to protonate any iridium phenyl complexes present in the solution. As an internal standard, 1 μL of mesitylene (0.864 mg, 0.00718 mmol) was added, producing an integration of the mesityl-H protons of 3.00. Normalization of the 3 mesitylene protons/mol of mesitylene relative to the 6 benzene-H₆ protons/mol of benzene (integration of 4.24) results in 0.005 07 mmol of benzene-H₆ produced. This resulted in 39.9% of benzene-H₆ relative to the amount of iridium starting material.

Acknowledgment. We thank the National Science Foundation (Grant No. CHE-0328121), Chevron Texaco Energy Technology Co., and Scripps Florida for financial support of this research. We thank Mr. Timothy Stewart and Prof. Robert Bau for X-ray structure determination.

Supporting Information Available: A CIF file and tables and figures giving X-ray structural data for **9**, ¹H NMR spectra for the stability studies of **6** in D₂O with and without added KOD, a plot of turnover number vs time for H/D exchange using **6** as a catalyst, a 1/[Py] plot for H/D exchange with **6**, ¹H NMR spectra for compounds **2–6** and **9–11**, and B3LYP xyz coordinates of transition states. This material is available free of charge via the Internet at <http://pubs.acs.org>.

(23) Young, K. J. H.; Meier, S. K.; Gonzales, J. M.; Oxgaard, J.; Goddard, W. A., III; Periana, R. A. *Organometallics* **2006**, *25*, 4734 (see the Supporting Information in this paper for an Excel spreadsheet).